# Structure formation in the Universe by exact methods

Andrzej Krasiński*
N. Copernicus Astronomical Centre, Polish Academy of Sciences,
Bartycka 18, 00 716 Warszawa, Poland, email: akr@camk.edu.pl

Charles Hellaby*
Department of Mathematics and Applied Mathematics,
University of Cape Town
Rondebosch 7701, South Africa, email: cwh@maths.uct.ac.za

**Abstract**

The evolution equations of the Lemaître-Tolman (LT) model are reformulated so that matter density $\rho_i$ or velocity $v_i$ at two times $t_i$, $i = 1, 2$ are the input data. Then, numerical examples of the LT models are constructed that evolve between a density or velocity distribution at $t_1$ = last scattering epoch and a structure at $t_2$ = the present time. The amplitude of the inhomogeneity at $t_1$ is within the limits implied by observations, and the final structure is a galaxy cluster, a void or a galaxy with a central black hole. It is shown that the initial velocity distribution plays an essential role in the formation of structures, the density distribution alone does not even determine whether the final structure will be a void or a condensation.

## 1 A new formulation of the evolution equations.

In the traditional approach to dynamics, one formulates the initial data (e.g. positions and velocities of particles) at a time $t_1$, then one uses the field equations to evolve the data to $t_2 > t_1$, and compares the calculated results at $t_2$ with observations or experiments. However, in cosmology the initial state at $t_1$ (taken, for example, to be at last scattering) is not accessible to observations. The observational data are collected at the final instant $t_2$, and only some of them can be projected back to $t_1$. Using the traditional approach, one assumes various data at $t_1$ and tries to "shoot" into the observed final state at $t_2$.

However, the evolution equations can be reformulated so that information from both $t_1$ and $t_2$ can be fed into the models. We present here such an approach to the Lemaître-Tolman (L-T) model [1, 2, 3]. We demonstrate numerical examples of evolution of small

*This research was supported by the Polish Research Committee grant no 2 P03B 060 17 and by a grant from the South African National Research Foundation. This is an abbreviated version of the talk given at the "Mathematics of Gravitation II" workshop in Warsaw in September 2003.

initial density or velocity fluctuations at $t_1$ = last scattering epoch to modern structures such as galaxy clusters and voids at $t_2$ = now. The reformulated equations have unique solutions under conditions that are easy to verify.

The L–T model has two disadvantages. Because of its spherical symmetry, we cannot take rotation into account. In consequence, the model does not apply to single galaxies, and is a rough approximation to galaxy clusters. The only objects to which the model can be applied are voids because for them it has been proved (by Newtonian methods) that spherical symmetry is a stable property [4]. Because of zero pressure, the model is unable to describe any hydro- or thermodynamics, and so is not applicable to the early Universe and to late stages of collapse of matter.

Among the advantages, our method yields structures reasonably similar to galaxy clusters and galaxies with central black holes from initial conditions that are in agreement with the CMB observations, and highlights the interplay between the density and velocity fluctuations. Using exact solutions of the Einstein equations, we can track the evolution of the structures up to the present and into the future, linear or nonlinear 'regimes' being irrelevant. We do have problems, though, with generating voids, see sec. 7.

# 2 The Lemaître-Tolman model.

The Lemaître-Tolman (L-T) model [1, 2] is a spherically symmetric nonstatic solution of the Einstein equations with a dust source [3]. Its metric is:

$$\mathrm{d}s^2 = \mathrm{d}t^2 - \frac{{R,_r}^2}{1+2E(r)}\mathrm{d}r^2 - R^2(t,r)(\mathrm{d}\vartheta^2 + \sin^2\vartheta \mathrm{d}\varphi^2), \tag{2.1}$$

where $E(r)$ is an arbitrary function, $R,_r = \frac{\partial R}{\partial r}$, and $R$ obeys the equation

$$ {R,_t}^2 = 2E + 2M/R + \frac{1}{3}\Lambda R^2, \tag{2.2}$$

where $\Lambda$ is the cosmological constant. Eq. (2.2) is a first integral of the Einstein equations, and $M(r)$ is another arbitrary function. The solution of (2.2) will depend on $t$ through the combination $(t - t_B(r))$, where $t_B(r)$ is one more arbitrary function – the position-dependent "bang time". The matter-density is:

$$\kappa\rho = \frac{2M,_r}{R^2 R,_r}, \qquad \text{where } \kappa = \frac{8\pi G}{c^4}. \tag{2.3}$$

It becomes singular where $\{R = 0, M,_r \neq 0\}$ and $\{R,_r = 0, M,_r \neq 0\}$. Both are curvature singularities. The first is the Big Bang. The second one is the shell-crossing singularity that can be avoided by a proper choice of the arbitrary functions [5].

In the following, we will assume $\Lambda = 0$. Then the solutions of eq. (2.2) are:

When $E < 0$:

$$R(t,r) = -\frac{M}{2E}(1 - \cos\eta),$$

$$\eta - \sin\eta = \frac{(-2E)^{3/2}}{M}(t - t_B(r)). \tag{2.4}$$

where $\eta$ is a parameter; when $E = 0$:

$$R(t,r) = \left[\frac{9}{2}M(t - t_B(r))^2\right]^{1/3}, \tag{2.5}$$

and when $E > 0$:

$$R(t,r) = \frac{M}{2E}(\cosh\eta - 1),$$

$$\sinh\eta - \eta = \frac{(2E)^{(3/2)}}{M}(t - t_B(r)). \tag{2.6}$$

Note that all the formulae given so far are covariant under arbitrary coordinate transformations $r = g(r')$. It will be convenient to use $r' = M(r)$ as the radial coordinate. This is allowed because we will consider regions of the Universe that are small compared to the radius of curvature, and so $M,_r > 0$. (The change of sign of $M,_r$ can occur when considering very large scales such as e.g. half the circumference of the closed $t =$ const space in the $k > 0$ Friedmann model.) Then:

$$\kappa\rho = 2/(R^2 R,_M) \equiv 6/(R^3),_M, \tag{2.7}$$

and this equation is easily inverted so that $R(t,r)$ is defined by a given $\rho(t,r)$:

$$R^3 = \int_0^M \frac{3c^2}{4\pi G\rho(t,x)}\mathrm{d}x \tag{2.8}$$

(the last equation results with the initial condition $R = 0$ at $M = 0$ which we assume).

# 3 Defining a model by initial and final profiles.

## 3.1 Part I: Density to density evolution.

We specify the density distributions at the instants $t = t_i$, $i = 1, 2$:

$$\rho(t_i, M) = \rho_i(M), \tag{3.1}$$

and calculate the corresponding $R(t_i, M)$ by eq. (2.8). Throughout the paper we assume $R,_t(t_1, M) > 0$. This assumption is dictated by the intended application of our results (structure formation in the Universe), but a similar investigation could be done for collapsing matter. For definiteness, we also assume $t_2 > t_1$ throughout.

### 3.1.1 $E > 0$.

We write out the evolution equations (2.6) at $t_1$ and $t_2$:

$$\begin{aligned} R_i(M) = R(t_i, M) &= \frac{M}{2E}(\cosh\eta_i - 1), \\ \sinh\eta_i - \eta_i &= \frac{(2E)^{(3/2)}}{M}\left[t_i - t_B(M)\right], \end{aligned} \tag{3.2}$$

and $R_2(M) > R_1(M)$ in consequence of $\rho(t_2, M) < \rho(t_1, M)$. Solving for $t_B$ at $t_1$ we get

$$t_B = t_1 - \frac{M}{(2E)^{3/2}} \left[\sqrt{(1 + 2ER_1/M)^2 - 1} - \mathrm{arcosh}(1 + 2ER_1/M)\right]. \tag{3.3}$$

We substitute this in (3.2) at $t_2$ and get

$$\sqrt{(1 + 2ER_2/M)^2 - 1} - \mathrm{arcosh}(1 + 2ER_2/M)$$
$$-\sqrt{(1 + 2ER_1/M)^2 - 1} + \mathrm{arcosh}(1 + 2ER_1/M) = [(2E)^{3/2}/M](t_2 - t_1). \tag{3.4}$$

This equation defines $E(M)$, and then (3.3) defines $t_B(M)$. These two functions then define the L–T evolution from $\rho(t_1, M)$ to $\rho(t_2, M)$. But does eq. (3.4) have any solutions, and if so, is the solution unique? For ease of calculations, let us denote:

$$x := 2E/M^{2/3}, \qquad a_i = R_i/M^{1/3}, \quad i = 1, 2;$$
$$\psi_H(x) := \sqrt{(1 + a_2 x)^2 - 1} - \mathrm{arcosh}(1 + a_2 x) - \sqrt{(1 + a_1 x)^2 - 1} + \mathrm{arcosh}(1 + a_1 x)$$
$$-(t_2 - t_1)x^{3/2}, \tag{3.5}$$

The problem is then: for what values of $a_2 > a_1$ and $t_2 > t_1$, does the equation $\psi_H(x) = 0$ have a solution $x \neq 0$? An elementary reasoning [6] leads to the conclusion that the equation has a solution if and only if the following inequality is fulfilled:

$$t_2 - t_1 < \frac{\sqrt{2}}{3}\left({a_2}^{3/2} - {a_1}^{3/2}\right), \tag{3.6}$$

and then the solution is unique. This inequality says that the expansion between $t_1$ and $t_2$ must have been faster than it would be in the $E = 0$ model.

The result above only shows the existence of a solution for a given value of $M$. Some initial conditions may lead to shell crossings, and these are not excluded by (3.6). But the criteria for the occurrence of shell crossings are well-investigated [5]. If shell crossings occur outside the range where the model is supposed to apply (e.g. before $t_1$), then they are no problem – the L–T model cannot describe those epochs anyway.

### 3.1.2 $E < 0$.

The evolution must be considered separately for the final state expanding (for which $\eta \in [0, \pi]$ in (2.4)) and for the final state recollapsing ($\eta \in [\pi, 2\pi]$ in (2.4)).

For the still-expanding final state, the variable $x$ and the $\psi$-function are:

$$x := -2E/M^{2/3},$$
$$\psi_X(x) := \arccos(1 - a_2 x) - \sqrt{1 - (1 - a_2 x)^2} - \arccos(1 - a_1 x) + \sqrt{1 - (1 - a_1 x)^2}$$
$$-(t_2 - t_1)x^{3/2}, \tag{3.7}$$

the definitions of $a_i$ being still (3.5).

The reasoning is analogous to the one for (3.5), but the arguments of arccos must have absolute values not greater than 1. This implies $x \leq 2/a_i$ for both $i$, and so, since $a_2 > a_1$

$$0 \leq x \leq 2/a_2, \tag{3.8}$$

which means: if there is any solution of $\psi_X(x) = 0$, then it will have the property (3.8). Eq. (3.8) is equivalent to $(R_{,t})^2 \geq 0$ at both $t_1$ and $t_2$.

Again, an elementary reasoning [6] leads to the conclusion that $\psi_X(x) = 0$ has a solution if and only if two inequalities are fulfilled at the same time:

$$\frac{\sqrt{2}}{3}\left({a_2}^{3/2} - {a_1}^{3/2}\right) < t_2 - t_1 \leq (a_2/2)^{3/2}\left[\pi - \arccos(1 - 2a_1/a_2) + 2\sqrt{a_1/a_2 - (a_1/a_2)^2}\right]. \tag{3.9}$$

With the inequalities fulfilled, the solution is unique. The first inequality means that the model must have expanded between $t_1$ and $t_2$ slower than the $E = 0$ model; the second inequality means that the final state is still earlier than the instant of maximal expansion.

As is seen from (2.1), the function $E$ must obey $E \geq -1/2$, or else the signature of the spacetime will become unphysical. This condition does not follow from (3.9) and has to be verified separately, together with the no-shell-crossing conditions.

For the recollapsing final state, $x$ is defined as in (3.9), but the $\psi$-function is:

$$\psi_C(x) := \pi + \arccos(-1 + a_2 x) + \sqrt{1 - (1 - a_2 x)^2} - \arccos(1 - a_1 x) + \sqrt{1 - (1 - a_1 x)^2} \\ -(t_2 - t_1)x^{3/2}. \tag{3.10}$$

The solution of $\psi_C(x) = 0$ exists if and only if

$$t_2 - t_1 \geq (a_2/2)^{3/2}\left[\pi - \arccos(1 - 2a_1/a_2) + 2\sqrt{a_1/a_2 - (a_1/a_2)^2}\right], \tag{3.11}$$

and then the solution is unique (see again Ref. [6] for details).

## 3.2 Part II: Velocity to density evolution.

A measure of velocity of expansion is $R_{,t}(t, M)/M^{1/3}$; it becomes constant in the Friedmann limit. Suppose that the initial state is specified by:

$$b_1(M) = R_{,t}(t_1, M)/M^{1/3}, \tag{3.12}$$

while the final state is specified by a density distribution $\rho(t_2, M)$. Does the scheme of the previous subsection still go through? It turns out it does, in a very similar way.

### 3.2.1 $E > 0$.

With the variables defined as in (3.5) and (3.12), the equation is $\Phi_H(x) = 0$, where

$$\Phi_H(x) := \sqrt{(1 + a_2 x)^2 - 1} - \sqrt{\left(\frac{{b_1}^2 + x}{{b_1}^2 - x}\right)^2 - 1} - \operatorname{arcosh}(1 + a_2 x) + \operatorname{arcosh}\left(\frac{{b_1}^2 + x}{{b_1}^2 - x}\right)$$

$$-x^{3/2}\left(t_2 - t_1\right). \tag{3.13}$$

Now the necessary and sufficient condition for the solvability of $\Phi_H(x) = 0$ is:

$$t_2 - t_1 < \frac{\sqrt{2}}{3}{a_2}^{3/2} - \frac{4}{3{b_1}^3}, \tag{3.14}$$

$$2/a_2 < {b_1}^2. \tag{3.15}$$

The second one is a necessary condition for the existence of a $t_2 > t_1$ obeying (3.14), and is equivalent to $R_2 > R_1$. With both inequalities fulfilled, the solution of $\Phi_H(x) = 0$ is unique. Eq. (3.14) is equivalent to (3.6) [7].

### 3.2.2 $E < 0$.

When the final state is still expanding, the necessary and sufficient condition for the existence of an L–T evolution between the two given states is:

$$\frac{\sqrt{2}}{3}{a_2}^{3/2} - \frac{4}{3{b_1}^3} < t_2 - t_1 \le (a_2/2)^{3/2}\left[\pi + \frac{b_1\sqrt{2a_2}}{a_2{b_1}^2/2 + 1} - \arccos\frac{a_2{b_1}^2/2 - 1}{a_2{b_1}^2/2 + 1}\right]. \tag{3.16}$$

This set of inequalities is equivalent to eq. (3.9). With the inequalities fulfilled, the solution of the corresponding equation (see [7]) is unique.

When the final state is recollapsing, the $E < 0$ evolution exists if and only if

$$t_2 - t_1 \ge (a_2/2)^{3/2}\left[\pi + \frac{b_1\sqrt{2a_2}}{a_2{b_1}^2/2 + 1} - \arccos\left(\frac{a_2{b_1}^2/2 - 1}{a_2{b_1}^2/2 + 1}\right)\right]. \tag{3.17}$$

## 3.3 Part III: Velocity to velocity evolution.

The given quantities are now:

$$b_i(M) = R_{,t}\left(t_i, M\right)/M^{1/3}, \qquad i = 1, 2. \tag{3.18}$$

We assume $b_1 > 0$ and $t_2 > t_1$. Then, the necessary and sufficient condition for the existence of an $E > 0$ evolution between the two states is:

$$0 < b_2 < b_1, \tag{3.19}$$

$$t_2 - t_1 > \frac{4}{3}\left(\frac{1}{{b_2}^3} - \frac{1}{{b_1}^3}\right). \tag{3.20}$$

The second inequality becomes more intelligible when it is rewritten as

$${b_2}^3 > \frac{{b_1}^3}{1 + \frac{3}{4}{b_1}^3\left(t_2 - t_1\right)}, \tag{3.21}$$

which means that an $E > 0$ evolution between the two states will exist provided the velocity of expansion at $t_2$ is greater than the velocity of expansion of the $E = 0$ model.

The necessary and sufficient condition for the existence of an $E < 0$ evolution when the final state is still expanding is the set consisting of (3.19) and

$$t_2 - t_1 < \frac{4}{3}\left(\frac{1}{{b_2}^3} - \frac{1}{{b_1}^3}\right), \tag{3.22}$$

which now implies that the expansion between $t_1$ and $t_2$ must have been slower than it would be in an $E = 0$ model.

When the final state is already recollapsing, we have $b_2 < 0$. Then the evolution exists for any values of $b_1 > 0$ and $b_2 < 0$, with no further conditions.

# 4 Transforming scales in the background.

We imagine that the structure at $t_2$ has accumulated its present mass by drawing matter in from the surroundings. Thus, a condensation (such as a galaxy cluster) will be enveloped in a region where the density is lower than the cosmic average, up to the distance $R_c$, called *compensation radius*, at which the total mass within $R_c$ is the same as it would be in a Friedmann (dust) model. Beyond $R_c$, the Friedmann background remains unperturbed.

For simplicity, we assume that the background outside $R_c$ is the $k = 0$ Friedmann model. We wish to know what angle would be subtended in the CMB sky by matter that today forms various objects. For this, we calculate the physical radius of the past null cone

$$L(t) = S\int_t^{t_0} \frac{1}{S}\,dt = 3c\,(t_0^{1/3} t^{2/3} - t). \tag{4.23}$$

Consequently, an observed angular scale of $\theta$ on the CMB sky has a physical size at the recombination time $t_1$ given by

$$L_1 = L(t)\,\theta = 3c\,(t_0^{1/3} t_1^{2/3} - t_1)\,\theta. \tag{4.24}$$

The present day size of the observed structure – assuming it doesn't collapse – is thus

$$L_2 = L_1 \frac{S_2}{S_1} \tag{4.25}$$

We assume that today's structures had not yet existed at $t = t_1$ – their matter was uniformly spread through the background. To calculate the radius occupied by that matter we take the present mass $M_2$ of the object under consideration and spread it over such a volume that the mean density in the object becomes equal to the mean background density at $t_2$. The radius of that region (call it "equivalent background radius", EBR) is

$$L_2 = \left(\frac{3M_2}{4\pi\rho_{b2}}\right)^{1/3}. \tag{4.26}$$

We then scale down this radius to $t_1$ by the law (4.25). The result is

$$\left(\frac{3M_2}{4\pi\rho_{b2}}\right)^{1/3}\left(\frac{t_1}{t_2}\right)^{2/3} = 3c\,(t_0^{1/3} t_1^{2/3} - t_1)\,\theta. \tag{4.27}$$

This relation was used to calculate the angles given in the table below [6].

| | Radius today (kpc) | Mass ($M_\odot$) | Density of sphere ($\rho_b$) | Angle on CMB sky (°) |
|---|---|---|---|---|
| star | $2 \times 10^{-11}$ | 1 | $2 \times 10^{29}$ | $8 \times 10^{-7}$ |
| globular cluster | 0.1 | $10^5$ | $2 \times 10^5$ | $4 \times 10^{-5}$ |
| galaxy | 15 | $10^{11}$ | $6 \times 10^4$ | $4 \times 10^{-3}$ |
| Virgo cluster | 2 000 | $2 \times 10^{13}$ | 5 | 0.02 |
| Virgo supercluster | 15 000 | $5 \times 10^{14}$ | 0.3 | 0.06 |
| Abell cluster (example) | 800 | $10^{15}$ | 4 000 | 0.08 |
| void | $6 \times 10^4$ | ? | | 0.4 |
| COBE resolution | $1.6 \times 10^6$ | $1.9 \times 10^{21}$ | (1) | 10 |
| BOOM/MAX resolution | $3.1 \times 10^4$ | $1.5 \times 10^{16}$ | (1) | 0.2 |

Thus, at the current best resolution, the only structures whose trace has a chance of appearing on the CMB sky are the voids. There are just no data to constrain the fluctuations at $t_1$ that will later develop into smaller structures such as clusters of galaxies.

# 5 Initial density and velocity fluctuations.

The current best estimate of the maximal value of $(\Delta T/T)_{\max}$, i.e. the amplitude of temperature anisotropies in the CMB radiation today, is

$$(\Delta T/T)_{\max} \approx 2.93 \times 10^{-6}, \tag{5.1}$$

and this is attained at the wavenumber $\ell \approx 200$, which corresponds to the radius of the fluctuation filling the angle $\alpha = 0.9°$ [8]. A volume that would develop into a galaxy cluster would be visible on the CMB sky at $\ell > 1800$, which corresponds to $\alpha < 0.9°$.

The currently accepted limit on the relative density fluctuation $\Delta\rho/\rho$ at $t_1$ is $10^{-5}$ [9]. To calculate the allowed relative velocity fluctuation we used the result by Dunsby [10]: the $(\Delta T/T)_{\max} \approx 2.93 \times 10^{-6}$ translates to $\Delta b/b\,(t_1) \approx 10^{-4}$.

No data exist on the *shape* of the density or velocity profiles at $t_1$ or on the spatial extent of the region that is perturbed at $t_1$. For the shape, we assumed simple functions. It turned out that the final outcome of evolution is sensitive to the initial velocity profile, see sec. 7. With the spatial extent, we assumed that the initial density perturbation for the formation of a galaxy cluster contained a mass of about 0.01 of the final mass.

# 6 Modelling a galaxy cluster.

We made the standard choice of units, in which $c = 1$ and $G = 1$. We chose the mass unit $1M_G = 10^{15} M_\odot$ for galaxy clusters and $1M_G = 55 \times 10^{15} M_\odot$ for voids. The associated units of distance ($L_G$) and time ($T_G$) are (recall: 1 pc = 3.26 light years = 3.09 $\times 10^{18}$ cm)

| | $1L_G$ | $1T_G$ |
|---|---|---|
| galaxy cluster | 47.84 pc | 156 yr |
| void | 2631 pc | 8582 yr |

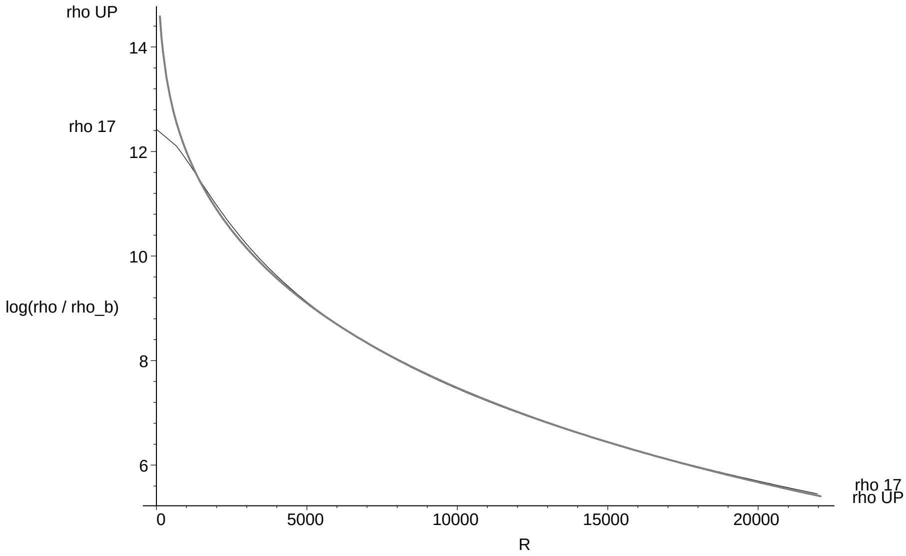


Figure 1: Comparison of the L–T density profile $\rho_{17}$ used for the Abell cluster model with the Newtonian Universal Profile.

One of the objects we chose to model was the galaxy cluster A2199 from the Abell catalogue. The following (Newtonian!) ‘universal profile’ is in use in astronomy [11]:

$$\rho(R) = \rho_b \frac{\delta}{(R/R_s)(1 + R/R_s)^2}, \tag{6.1}$$

where $\rho_b$ ($= 8 \times 10^{-30}$ g/cm$^3$) is the average density in the Universe, $\delta$ ($=$ 77 440) is a dimensionless factor and $R_s$ ($= 3457 L_G = 1.65 \times 10^5$ pc $= 5.11 \times 10^{18}$ km) is a scale distance. This profile is said to apply for $R$ changing by two orders of magnitude [11].

For our procedure, we need the density given as a function of mass.[1] The calculation $\rho(R) \to M(R) \to R(M) \to \rho(M)$ can always be done numerically, but it is more instructive to have exact explicit formulae. We therefore approximated the ’universal profile’ by the following $\rho(M)$ profile (where now $\rho$ is meant to be that of (2.3)):

$$\rho_{17}(R) = \rho_b \frac{B_2}{1 + \mathrm{e}^{\sqrt{M/\mu_2}}}, \tag{6.2}$$

in which $B_2 = 498500$ and $\mu_2 = 0.07144 M_G$. Fig. 1 shows the profiles (6.1) and (6.2).

For the initial profile at $t_1$ we chose

$$\rho/\rho_b = \begin{cases} 1 + A_1 \left[1 + \cos\left(\frac{100\pi M}{M_c}\right)\right] & \text{for} \quad M < M_c/100 \\ 1 & \text{for} \quad M > M_c/100, \end{cases} \tag{6.3}$$

where $A_1 = 0.000015$ and $M_c = 1.182 M_G$ is the compensation mass, see Fig. 2.

[1]Note that the relation between mass and density in the L-T model, eq. (2.3), is different from the flat-space relation $\mathrm{d}M/\mathrm{d}R = 4\pi\rho R^2$. We carried over eq. (6.1) to relativity with the hope that it is a good approximation at low densities. However, a completely self-consistent approach would require re-interpretation of all the relevant astronomical observations against the L-T model.

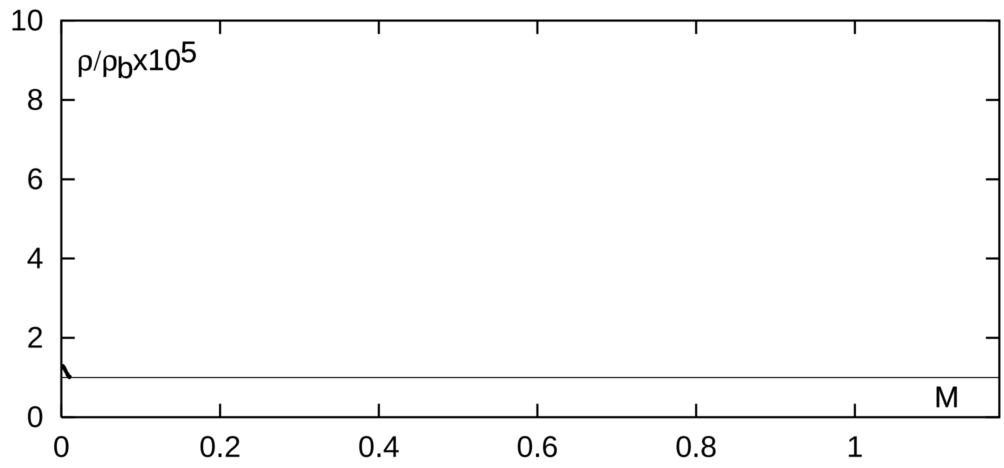


Figure 2: The initial density profile used for the Abell cluster model.

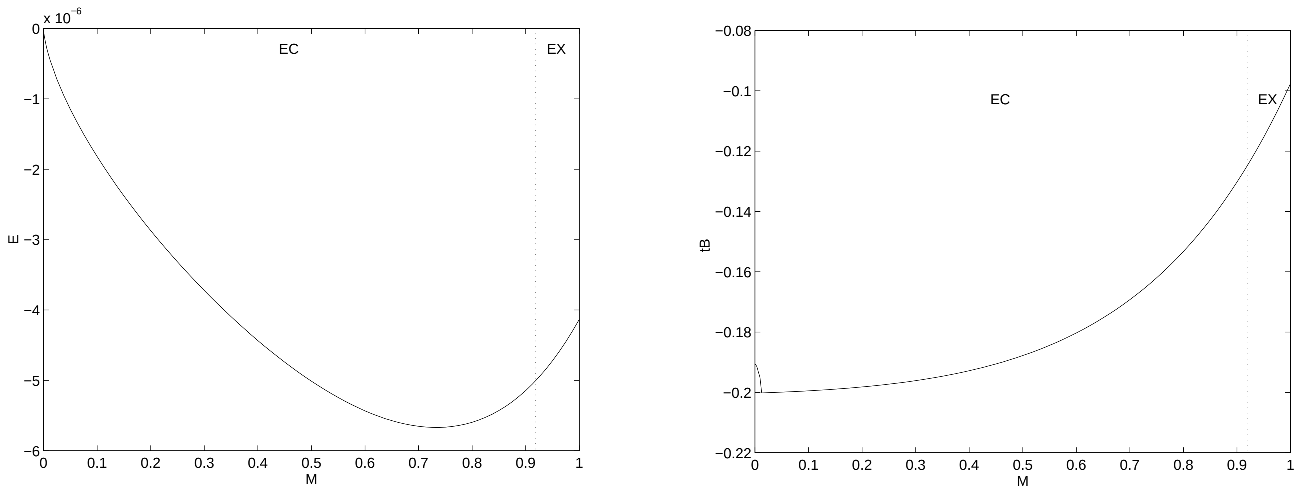


Figure 3: The function $E(M)$ (left) and the bang function (right) for the Abell cluster model. Explanation in the text.

Fig. 3, left graph shows the numerically calculated function $E(M)$ corresponding to the profiles shown in Figs. 1 and 2. It is everywhere negative, which means that all matter within the model will eventually collapse. The dotted vertical line separates matter that is already recollapsing at $t_2$ (left) from matter that is still expanding at $t_2$. Fig. 3, right graph shows $t_B(M)$ for the same evolution. The difference in age between the central part of the cluster and its outer part is approx. $0.1T_G \approx 15.6$ years, i.e. this Big Bang is almost simultaneous. However, strictly speaking, the increasing function $t_B(M)$ implies a shell-crossing. It will occur before $t_B$, where the model does not apply anyway.

Given $E(M)$ and $t_B(M)$, one can calculate the associated distribution of velocity $b_1(M) = R,_t(t_1, M)$ at $t_1$. This is shown in Fig. 4. The relative amplitude of the initial velocity at the center is about $5 \times 10^{-4}$, which is within the observational limits (but we recall that these limits correspond to objects of much larger size).

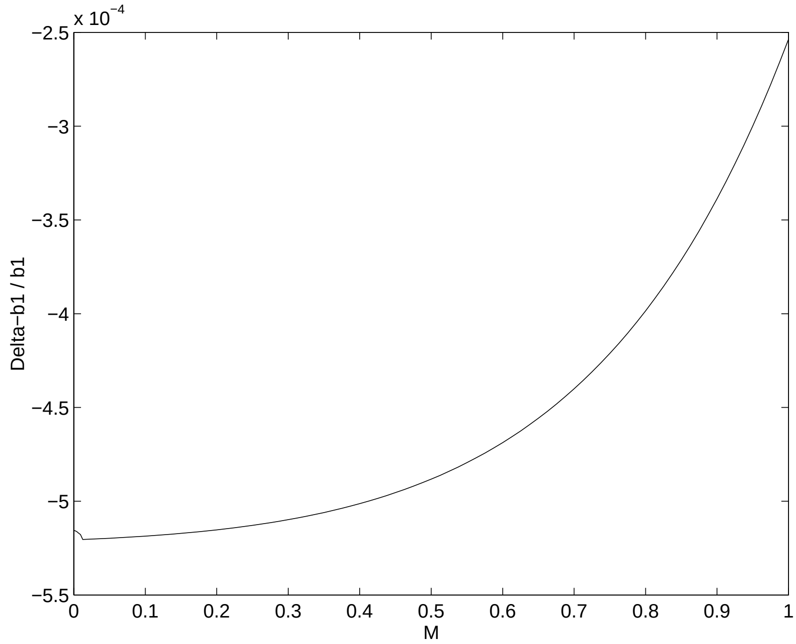


Figure 4: The implied initial velocity distribution for the Abell cluster model. Explanation in the text.

# 7 Modelling a void.

For modelling a void formation we used the two profiles introduced in Fig. 5. Profile 18 created a shell crossing immediately after $t_2$. Profile 20 is:

$$\rho_{20} = \rho_b \frac{B_2 {\mu_2}^2 + M^2}{{\mu_2}^2 + (M - \mu_2)^2}, \tag{7.1}$$

with $B_2 = 0.3873$ and $\mu_2 = 0.2475 M_G$. The radius of the low-density region is about 60 Mpc. We tried to generate this final profile from the initial velocity profile given by

$$\frac{R,_t}{(R,_t)_b} = 1 + A_1 \left[1 + \cos\left(\frac{\pi M}{M_c}\right)\right], \tag{7.2}$$

where $A_1 = 5 \times 10^{-5}$ and $M_c = 1 M_G$, see Fig. 6.

Fig. 7 shows the resulting $t_B(M)$ (left), and the implied $(\Delta\rho/\rho)(t_1)$ (right). The age-difference between the central point and the outer edge of the void is approx. $4.25 \times 10^5$ years, which would be acceptable. However, the density amplitude at $t_1$ is 0.16 – too large by 4 orders of magnitude. It is sensitive not just to the velocity amplitude at $t_1$, but also to the velocity profile assumed. We tried several initial distributions of density and velocity with the same final $\rho_{20}$, and we had a better result with a flat initial density. This is shown in Fig. 8 – the implied velocity amplitude at $t_1$ is $(\Delta b/b)(t_1) \approx 0.03$, which differs from the observationally allowed value by two orders of magnitude. (The age difference between the center and edge is this time approx. 85 000 years.)

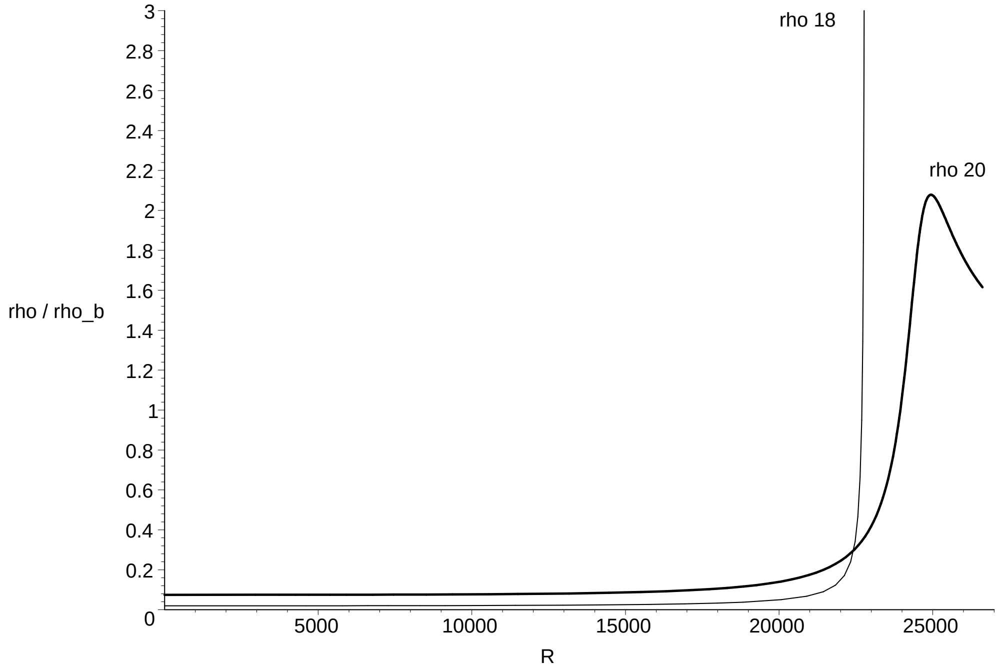


Figure 5: The density profiles at $t_2$ assumed for void models.

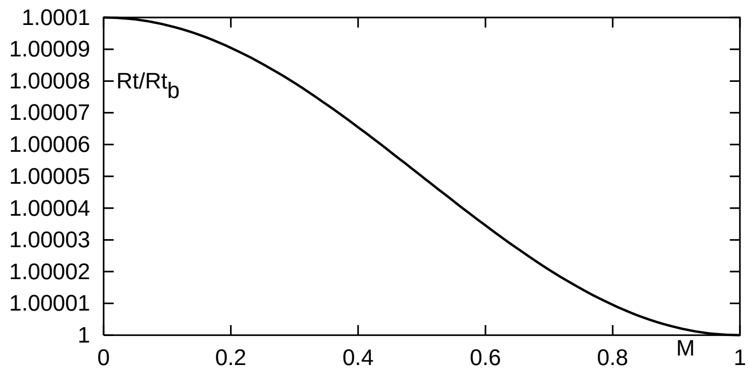


Figure 6: The initial velocity profile at $t_1$ assumed for a void model.

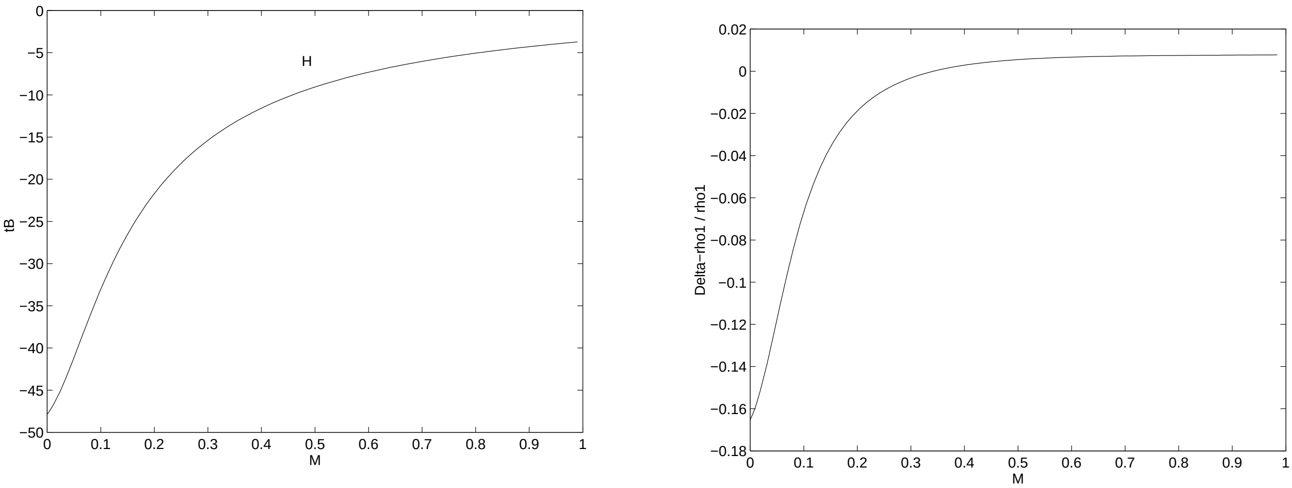


Figure 7: The bang time function (left) and the implied relative density amplitude $\Delta\rho/\rho$ at $t_1$ (right) for the void profile $\rho_{20}$, generated out of a velocity perturbation. The letter "H" means that this portion of matter will be ever-expanding (hyperbolic).

# 8 Results of some other numerical experiments.

For the evolution from a homogeneous initial density to a galaxy cluster (another profile approximating the "Universal Profile" [7]) we obtained the velocity amplitude at $t_1$

$$(\Delta b/b)(t_1)|_{\max} = 5.2 \times 10^{-4}, \tag{8.3}$$

which is on the border of the observationally implied range. This means that a pure velocity perturbation can very nearly produce a galaxy cluster.

For the evolution from a homogeneous initial velocity to a galaxy cluster (same final profile as above) we obtained the associated density amplitude at $t_1$

$$(\Delta\rho/\rho)(t_1)|_{\max} = 12 \times 10^{-3}, \tag{8.4}$$

which differs from the observationally allowed value by 3 orders of magnitude. Hence, velocity perturbations generate structures much more efficiently than density perturbations.

We demonstrated that a smooth evolution can take an initial condensation to a void (see also Ref. [12]). Thus the initial density distribution does not determine the final structure that will emerge from it; the velocity distribution can obliterate the initial setup.

We considered a condensation evolving to a spherical galaxy with a black hole around its center. We allowed for two possibilities for the black hole: that it formed in consequence of collapse, or that it was a wormhole created in the Big Bang. The final density profile was in both cases taken the same as for the M87 galaxy, and the mass hidden inside the apparent horizon was taken equal to what the observations imply for the mass contained inside the M87 black hole. The initial velocity profile was assumed homogeneous, since

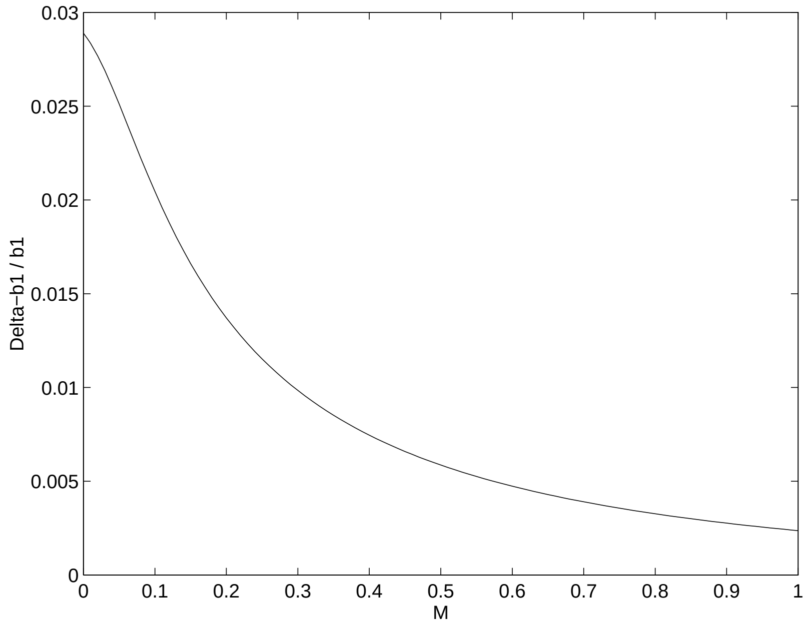


Figure 8: The implied relative velocity amplitude at $t_1$ for the void profile $\rho_{20}$, created out of a homogeneous density at $t_1$.

at the scale of a single galaxy there are no observational data on the fluctuations of the CMB temperature. The initial density amplitude came out to be $0.6 \times 10^{-5}$ – well below the value that the observations allow at larger angular scales. This investigation will be published separately [13].

# 9 Conclusions

The method presented in sec. 3 works, with limitations resulting from spherical symmetry, but needs further refinement. In particular, the proper shape of the velocity profile at $t_1$ for void formation is still unknown.

Velocity perturbations are more efficient in generating structures than density perturbations. The "gravitational instability paradigm" thus needs a revision. This point is strengthened by the fact that an initial condensation can evolve into a void.

The angular distribution of the CMB temperature must be known at much finer scales before any models of structure formation can be truly tested against observations. The current best resolution of $0.2^\circ$ is to be compared with the approximate angular sizes of the portions matter that will go into a galaxy cluster, $0.08^\circ$, and into a single galaxy, $0.004^\circ$.

More general exact cosmological solutions will be needed to attempt exact modelling. An additional unsatisfactory feature of the spherically symmetric models used here is that once matter starts collapsing, it will keep collapsing to a singularity. In real objects, rotation can prevent collapse for a much longer time.

[1] G. Lemaître, *Ann. Soc. Sci. Bruxelles* **A53**, 51 (1933); reprinted in *Gen. Rel. Grav.* **29**, 641 (1997).

[2] R. C. Tolman, *Proc. Nat. Acad. Sci. USA* **20**, 169 (1934); reprinted in *Gen. Rel. Grav.* **29**, 935 (1997).

[3] A. Krasiński, "*Inhomogeneous Cosmological Models*", Cambridge U P (1997).

[4] H. Sato, K. Maeda, *Progr. Theor. Phys.* **70**, 119 (1983).

[5] C Hellaby, K. Lake, *Astrophys. J.* **290**, 381 (1985) [+ erratum: *Astrophys. J.* **300**, 461 (1985)].

[6] A. Krasiński and C. Hellaby, *Phys. Rev.* **D65**, 023501 (2002).

[7] A. Krasiński and C. Hellaby, *More examples of structure formation in the Lemaître–Tolman model.* gr-qc 0303016, in press in *Phys. Rev.* **D**.

[8] W. Hu, webpage: http://background.uchicago.edu/~whu/physics/tourpage.html

[9] T. Padmanabhan, *Cosmology and Astrophysics through problems*, Cambridge U P, 1996.

[10] P.K.S. Dunsby, *Class. Q. Grav.* **14**, 3391-3405 (1997).

[11] J. F. Navarro, C. S. Frenk and S. D. M. White, *Mon. Not. Roy. Astr. Soc.* **275**, 720 (1995).

[12] N. Mustapha and C. Hellaby, *Gen. Rel. Grav.* **33**, 455 (2001).

[13] A. Krasiński, C. Hellaby, *Formation of a galaxy with a central black hole in the Lemaître–Tolman model*, to be submitted.